

Straggling of an extended charge distribution in a partially degenerate plasma

A. Bret and C. Deutsch

*Laboratoire de Physique des Gaz et des Plasmas and Groupement de Recherches, Bâtiment 212,
Université de Paris XI, 91405 Orsay Cedex, France*

(Received 10 May 1993)

The straggling of pointlike and extended nonrelativistic charged particles stopped in a partially degenerate electron fluid is considered within the random-phase approximation. High- and low-projectile-velocities V are given specific attention, as well as classical and fully degenerate target plasmas. The straggling of diclusters randomly orientated with respect to V is also considered.

PACS number(s): 52.25.Tx, 34.50.Bw, 36.40.+d

I. INTRODUCTION

The stopping of extended charges and cluster of charges in an arbitrarily degenerate plasma has already been given recent attention [1] (Ref. [1] is hereafter referred to as paper I).

This is a topic of obvious significance for a quantitative understanding of beam-target interaction in the context of particle driven fusion [2] for instance. So, the present work is a natural sequel to paper I, where nonrelativistic ion stopping of extended charges and diclusters in partially degenerate plasmas have been investigated at some length. Here, we focus attention on the straggling quantity, which allows one to put an estimate on the inherent uncertainty of the stopping power.

The paper is organized as follows. The random-phase approximation (RPA) [3,5] formulation for estimating straggling at any temperature is outlined in Sec. II.

Low-velocity behaviors are detailed in Sec. III and previously existing limits at high and low temperature are recovered. Then the RPA dielectric function is approached through a plasmon-pole expression. One thus derives analytic expressions for plasmon and binary contributions to the straggling of pointlike and extended charges (Sec. IV). Section V is devoted to an extension of these results to dicluster stopping of a pair of randomly orientated charges.

II. STRAGGLING AT FINITE TEMPERATURE

To start with a fully quantum-mechanical framework, we implement the dynamical structure formalism [6].

Such an approach essentially relies on calculating the probability that the ion projectile loses an energy $\hbar\omega$ in a time interval dt . From a functional analysis point of view, stopping power appears as a first moment in ω , and

$$\Omega^2 = \frac{2e^2}{\pi\hbar V^2} \int_0^\infty \frac{dk}{k} |n(k)|^2 \int_0^{kV} d\omega (\hbar\omega)^2 \text{Im} \left[-\frac{1}{\epsilon(k, \omega)} \right] [2N(\omega) + 1], \tag{6}$$

for straggling.

The dependence on temperature (T dependence) essentially lies in $\epsilon(\mathbf{k}, \omega)$ and $N(\omega)$. Introducing the dimensionless Lindhard variables

straggling as the second one. This observation makes it useful to consider the collision cross section

$$R(\mathbf{q}, \omega) = \frac{2\pi}{\hbar^2} |eV(\mathbf{q})|^2 S(\mathbf{q}, \omega), \tag{1}$$

with impulse transfer $\hbar\mathbf{q}$. $\hbar\omega$ and $\hbar\mathbf{q}$ satisfy $\hbar\omega = \hbar\mathbf{q} \cdot \mathbf{V} + \hbar^2 q^2 / 2M$ and $V(q) = 4\pi Z e q^{-2}$, for a projectile ion of total charge Z . If the latter corresponds to a local charge density $n(\mathbf{r})$, fulfilling $Z = \int d^3\mathbf{r} n(\mathbf{r})$, then $V(q)$ becomes

$$V(q) = \frac{4\pi e n(\mathbf{q})}{q^2}, \tag{2}$$

$n(\mathbf{q})$ being the $n(\mathbf{r})$ Fourier transform. On the other hand, the dynamic structure factor $S(\mathbf{q}, \omega)$ is directly connected to the dielectric function $\epsilon(\mathbf{q}, \omega)$ through

$$S(\mathbf{q}, \omega) = \frac{\hbar q^2}{4\pi e^2} N(\omega) \text{Im} \left[-\frac{1}{\epsilon(\mathbf{q}, \omega)} \right], \tag{3}$$

in terms of the Planck distribution

$$N(\omega) = \frac{1}{e^{\hbar\omega/k_B T} - 1}. \tag{4}$$

For a projectile with mass $M \gg m_e$, the recoil energy $\hbar^2 q^2 / 2M$ may be neglected. Let us pose $\omega = \mathbf{q} \cdot \mathbf{V}$.

To simplify further derivations, we restrict from now to a spherically symmetric $n(\mathbf{r}) = n(r)$. A parity argument also allows one to use $N(\omega) + N(-\omega) = -1$, so that one gets simultaneously

$$\frac{dE}{dx} = \frac{2e^2}{\pi V^2} \int_0^\infty \frac{dk}{k} |n(k)|^2 \int_0^{kV} \omega d\omega \text{Im} \left[-\frac{1}{\epsilon(k, \omega)} \right], \tag{5}$$

for stopping and

$$Z = \frac{k}{2k_F}, \quad u = \frac{\omega}{kV_p}, \quad k_F = (3\pi^2 N_e)^{1/3}, \quad V_F = \frac{\hbar k_F}{m_e}$$

(N_e denotes electron density in number) enables us to rewrite Eq. (6) under the form $[\chi^2 = \alpha r_S / \pi, r_S = (\frac{4}{3}\pi N_e)^{-1/3} a_0^{-1}, \alpha = (9\pi/4)^{-1/3}]$

$$L\Omega = \frac{12}{\pi\chi^2} \left[\frac{V_F}{V} \right] \int_0^{V/V_F} u^2 du \int_0^\infty Z^2 |n(2k_F Z)|^2 \text{Im} \left[-\frac{1}{\epsilon(Z, u)} \right] [2N(z, u) + 1] dz, \quad (7)$$

where

$$N(Z, u) = [e^{4uZ/T_e} - 1]^{-1}. \quad (8)$$

The discussion developed in paper I for the critical distances of a given system of charges applies here again. So, the maximum size that a charge may have and be still taken pointlike with respect to the stragglings effect is $\hbar/2m_e(V + V_e)$. V_e is the average target electron velocity.

On the other hand, there exists a minimum distance between two charges, so that dicluster stragglings appears as a sum of two one-particle stragglings. It is given either by the plasma static screening length at low velocity ($V \ll V_e$), or the dynamic screening length V/ω_p at high velocity ($V \gg V_e$). ω_p denotes electron plasma frequency $(4\pi N_e e^2/m)^{1/2}$.

III. LOW-VELOCITY BEHAVIORS

The integrand in Eq. (6) is essentially nonvanishing for $\hbar\omega \ll k_B T$, with $[2N(\omega) + 1] \approx 2k_B T / \hbar\omega$.

Stragglings (6) thus reproduces the well-known approximation

$$\Omega^2 \approx 2k_B T \frac{dE}{dx}, \quad (9)$$

valid at low velocity, and often used in diagnostics of tokamak plasmas. Former studies [1] of the dielectric function show that in Eq. (7), the largest Z value is

$$L\Omega \approx \frac{12}{\pi} \left[\frac{V}{V_F} \right]^2 \int_0^\infty \frac{Z^4 |n(2k_F Z)|^2 dZ}{[Z^2 + \chi^2 f_1(Z, 0)]^2} \int_0^{V/V_F} u^2 \left[\frac{\partial f_2}{\partial u} \right]_{u=0} [2N(Z, u) + 1] du, \quad (14)$$

where

$$\left[\frac{\partial f_2}{\partial u} \right]_{u=0} = \frac{\mu}{2} \frac{1}{1 + e^{(Z^2 - \gamma)T_e}}, \quad \gamma = \beta\mu. \quad (15)$$

When $T \rightarrow 0, N \rightarrow 0$, Eq. (14) yields the limit

$$L\Omega_{T=0} = \frac{3}{2} \left[\frac{V}{V_F} \right]^2 \int_0^1 \frac{Z^4 |n(2k_F Z)|^2 dZ}{[Z^2 + \chi^2 f_1(Z, 0)]^2}, \quad (16)$$

quadratic in V , while the classical limit [Eq. (9)] is linear in V .

IV. HIGH VELOCITY

To ease technical manipulations, we shall restrict the discussion to a plasmon-pole approximation in space (Z, u) of the Lindhard variables [5].

$Z_m = V/V_F + V_e/V_F$. Equation (9) is then valid for

$$4Z_m \frac{V}{V_F} \ll T_e = \frac{T}{T_F} \quad \text{or} \quad 2V(V + V_e) \ll \frac{k_B T}{m_e}, \quad (10)$$

which yields

$$V \ll \frac{V_e}{2} \left[\left[1 + \frac{2k_B T}{m_e V_e^2} \right]^{1/2} - 1 \right]$$

with the classical limit ($k_B T \approx \frac{1}{2} m_e V_e^2$)

$$V \ll 0.205 V_e, \quad (11)$$

and the opposite degenerate limit ($k_B T \ll \frac{1}{2} m_e V_e^2$)

$$V \ll \frac{T}{4T_F} V_e, \quad (12)$$

making it clear that approximation (9) is indeed useless for a fully degenerate target. So, the case $T=0$ should be treated separately. This is achieved through a limited expansion of Eq. (7) around $u=0$.

Returning to the dielectric function expression

$$\epsilon(\mathbf{k}, \omega) = 1 - V(\mathbf{k}) \chi^0(\mathbf{k}, \omega), \quad (13)$$

explained later on in dimensionless form with $[\chi^2 = \alpha r_S / \pi, r_S = (\frac{4}{3}\pi N_e)^{-1/3} a_0^{-1}, \text{ and } \alpha = (9\pi/4)^{-1/3}]$.

At any temperature, in the low-velocity limit, one gets

Let us recall the dispersion relation for the resonant part

$$Z_r^2 = \frac{\chi^2}{3u^2} \quad (17)$$

and the sum rule

$$\int_0^\infty u du \text{Im} \left[\frac{1}{\epsilon(Z, u)} \right] = \frac{\pi\chi^2}{6Z^2}. \quad (18)$$

Restricting in plane (Z, u) to the above resonance curve and the line $Z=u$, while retaining a balance between collective and binary collision contribution through the sum rule (18), provides us with a plasmon-pole approximation [7]

$$\text{Im} \left[-\frac{1}{\epsilon(Z, u)} \right] \cong \frac{\pi\chi^2}{6uZ^2} \left[\delta \left[Z - \frac{\chi}{\sqrt{3u}} \right] Y(Z_1 - Z) + \delta(Z - u) Y(Z - Z_1) \right], \quad (19)$$

in terms of the Heaviside function $Y(x)$ and delta function $\delta(x)$. Z_1 refers to the highest Z_r value at finite temperature, so

$$Z_1 = \frac{\chi}{\sqrt{3A_0(T_e)}}, \quad A_0(T_e) = \frac{V_e}{V_F}.$$

A. Pointlike charges

According to Eq. (19), let us split Eq. (7) into a plasmon part and a binary collisions one, so that

$$L\Omega_{\text{pla}} = \frac{2Z^2\chi}{\sqrt{3}} \left[\frac{V_F}{V} \right]^2 \ln \left[\frac{V}{V_e} \right] [2N(\omega_p + 1)], \quad (20a)$$

$$L\Omega_{\text{coll}} = Z^2 \left[\frac{V_F}{V} \right]^2 \left[\left[\frac{V}{V_F} \right]^2 - \frac{Z_1^2}{2} \right] + Z^2 \frac{T_e}{2} \left[\frac{V_F}{V} \right]^2 \Lambda, \quad (20b)$$

where $\Lambda = \ln[(1 - e^{-2m_e V^2/k_B T}) / (1 - e^{-C^2})]$, N is the Planck function (4), while

$$C^2 = \left[\frac{\hbar\omega_p}{2k_B T} \right]^2 \frac{k_B T}{\frac{1}{2}m_e V_e^2}, \quad (21)$$

qualifies the T behavior. When $C \rightarrow \infty$, T -correcting terms turn negligible. Condition $C=1$ yields, respectively, a classical limit ($m_e V_e^2 \cong 2k_B T$)

$$\log_{10}(k_B T) = \frac{\log_{10}(N_e)}{2} - 6.66$$

and a degenerate one ($V_e = V_F$)

$$k_B T = 0.3664 N_e^{13} e^2$$

identical to the line $\lambda_{\text{Debye}} = R_{\text{Landau}}$ with $\lambda_{\text{Debye}} = (k_B T / 4\pi N_e e^2)^{1/2}$ and $R_{\text{Landau}} = e^2 / k_B T$.

$C=1$ is drawn in diagram (T, N_e) in Fig. 1 as a thick line. Within the RPA domain, classical plasmas are located in a region fulfilling $C \ll 1$. On the other hand, most of quantum plasmas fulfill $C \gg 1$. There exists also a domain where $T < T_F$ and $C < 1$ are simultaneously fulfilled. Regrouping altogether the two contributions (20) yields the asymptotic expansion

$$L\Omega = Z^2 + \frac{2Z^2\chi}{\sqrt{3}} \left[\frac{V_F}{V} \right]^2 \ln \left[\frac{V}{V_e} \right] \times \{ [2N(\omega_p) + 1] + \mathcal{O}(V^{-2}) \}. \quad (22)$$

The first term in the right-hand side represents close collisions contribution at $T=0$, with practically no T

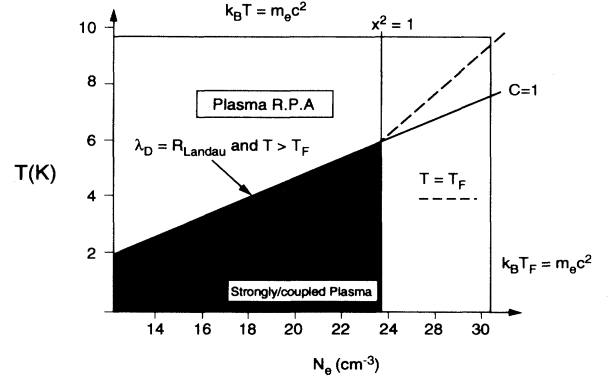


FIG. 1. Plane density temperature with temperature parameter C [Eq. (21)], line $\lambda_D = R_{\text{Landau}}$, and domains of various approximations.

correction. On the other hand, T corrections to plasmon straggling turn as large as the $T=0$ quantity itself.

B. Extended charge straggling

The low-velocity situation has already been addressed in Sec. III. So, we now concentrate on a projectile with a velocity $V \gg V_e$. Through Eq. (19), one can establish the respective extended charge contributions,

$$L\Omega_{\text{pla}}^{\text{ext}} = \frac{2\chi}{\sqrt{3}} \left[\frac{V_F}{V} \right]^2 [2N(\omega_p) + 1] \int_{Z_0}^{Z_1} \frac{|n(2k_F Z)|^2}{Z} dZ \quad (23)$$

and

$$L\Omega_{\text{coll}}^{\text{ext}} = 2 \left[\frac{V_F}{V} \right]^2 \int_{Z_1}^{V/V_F} Z |n(2k_F Z)|^2 \times \left[1 + \frac{2}{e^{4Z^2/T_e} - 1} \right] dZ, \quad (24)$$

where $Z_0 = \chi V_F / \sqrt{3V}$ and $Z_1 = (\chi / \sqrt{3}) A_0$.

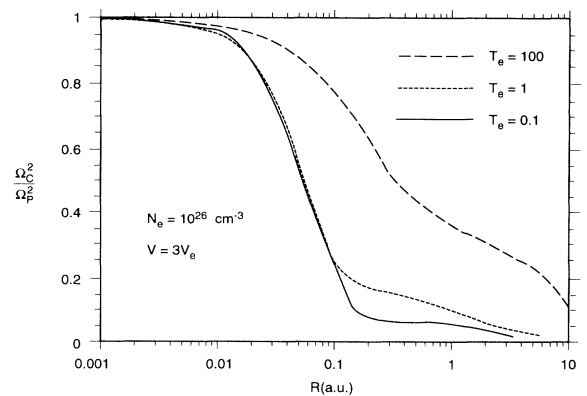


FIG. 2. Ratio of correlated to pointlike straggling Ω_c^2 / Ω_p^2 at high projectile velocity [Eqs. (27) and (28)].

V. DICLUSTER STOPPING

Let us consider a pair of charges Z_1e and Z_2e located at a relative distance \mathbf{R} . Taking averages over all relative orientations, one is led to introduce [8,9]

$$|n(k)|^2 = Z_1^2 + Z_2^2 + 2Z_1Z_2 \frac{\sin kR}{kR}, \quad (25)$$

in Eq. (6), so that

$$\Omega^2 = (Z_1^2 + Z_2^2)\Omega_p^2 + 2Z_1Z_2\Omega_c^2, \quad (26)$$

with

$$\Omega_p^2 = \frac{2e^2}{\pi\hbar V^2} \int_0^\infty \frac{dk}{k} \int_0^{kV} d\omega (\hbar\omega)^2 \text{Im} \left[-\frac{1}{\epsilon(k, \omega)} \right] [2N(\omega) + 1], \quad (27)$$

and

$$\Omega_c^2 = \frac{2e^2}{\pi\hbar V^2} \int_0^\infty \frac{dk}{k} \frac{\sin(kR)}{kR} \int_0^{kV} d\omega (\hbar\omega)^2 \text{Im} \left[-\frac{1}{\epsilon(k, \omega)} \right] [2N(\omega) + 1] \quad (28)$$

for pointlike and correlated contributions, respectively.

A. High velocity

In the high-velocity regime, Eqs. (23)–(24) become [$\text{sinc}x = (\sin x)/x$]

$$L\Omega_{\text{pla}}^{\text{ext}} = \frac{2\chi}{\sqrt{3}} \left[\frac{V_F}{V} \right]^2 [2N(\omega_p) + 1] \int_{Z_0}^{Z_1} \frac{|\text{sinc}(2k_F R Z)|^2}{Z} dZ \quad (29)$$

and

$$L\Omega_{\text{coll}}^{\text{ext}} = 2 \left[\frac{V_F}{V} \right]^2 \int_{Z_1}^{V/V_F} Z \text{sinc}(2k_F R Z) \left[1 + \frac{2}{e^{4Z^2/T_e} - 1} \right] dZ.$$

The plasmon part is explained with

$$H(x) = \text{Ci}(x) - \frac{\sin x}{x},$$

where $\text{Ci}(x)$ is the integral cosine, as

$$L\Omega_{\text{pla}}^{\text{ext}} = \frac{2\chi}{\sqrt{3}} \left[\frac{V_F}{V} \right]^2 [2N(\omega_p) + 1] \left[H \left[\frac{R\omega_p}{V} \right] - H \left[\frac{R}{\lambda_S} \right] \right]. \quad (30a)$$

λ_S is the appropriate screening length pertaining to a given plasma degeneracy. The collisional part is expressed by

$$L\Omega_{\text{coll}}^{\text{ext}} = 2 \left[\frac{V_F}{V} \right]^2 \left[\frac{\cos \left[\frac{R}{\lambda_S} \right]}{(2k_F R)^2} - \frac{\cos \left[\frac{R}{R_0} \right]}{(2k_F R)^2} \right] + \left[\frac{V_F}{V} \right]^2 \frac{T_e}{2} \int_c^{(2m_e V^2/k_B T)^2} \frac{\sin(\alpha R u)}{\alpha R u} \frac{2u du}{e^{u^2} - 1} \quad (30b)$$

with $R_0 = \hbar/2m_e V$. C is defined by Eq. (21) and $\alpha = T_e^{1/2} k_F$.

The second term in the right-hand side of Eq. (30b) accounts for T corrections of the correlated contribution to the straggling.

In the high-velocity limit $V \gg V_e$, the upper limit of the quadrature may be taken as infinity, up to a very good approximation. For $C > 1$, the corresponding contribution is $\sim e^{-C^2}$. When $C \ll 1$, the given term becomes a constant $\sim \ln(C)$.

The corresponding straggling contribution remains negligible compared to the close collisions one at $T=0$.

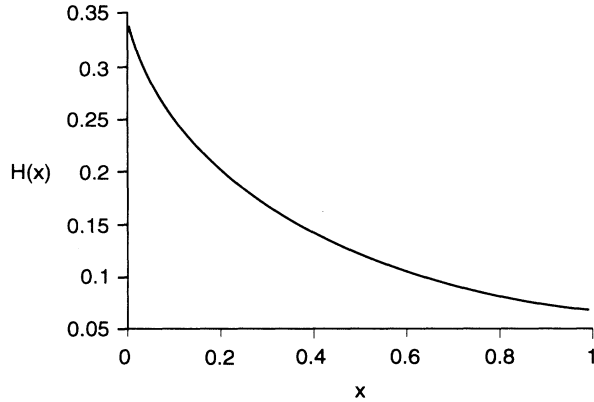
When $R \gg \omega_p/V$, one witnesses $L\Omega_{\text{coll}}^{\text{ext}} \ll L\Omega_{\text{pla}}^{\text{ext}}$, and

$$L\Omega^{\text{ext}} \cong -\frac{2\chi}{\sqrt{3}} \left[\frac{V_F}{V} \right]^2 [2N(\omega_p) + 1] \frac{\cos(R\omega_p/V)^2}{(R\omega_p/V)}. \quad (31)$$

The ratio Ω_c^2/Ω_p^2 of Eq. (27) to Eq. (28) is shown in Fig 2.

B. Low velocity and $T=0$

Let us rewrite Eq. (16) with $|n(2k_F Z)|^2 = \sin kR/kR$ and evaluate the quadrature

FIG. 3. Function $H(x)$ [Eq. (34)].

$$L_c(\Omega_T=0) = \frac{3}{2} \left[\frac{V}{V_F} \right]^2 \int_0^1 \frac{Z^4 \text{sinc}(2k_F R Z)}{[Z^2 + \chi^2 f_1(Z,0)]^2} dZ, \quad (32)$$

where

$$f_1(Z,0) = \frac{1}{2} \left[1 + \frac{1-Z^2}{2Z} \ln \left| \frac{Z+1}{Z-1} \right| \right]$$

is the Lindhard function. Equation (32) may be worked out to display a small $R \ll k_F^{-1}$ interparticle limit with

$$L_c(\Omega_T=0) \cong L_p(\Omega_T=0) - (k_F R)^2 \left[\frac{V}{V_F} \right]^2 H(\chi^2), \quad (33)$$

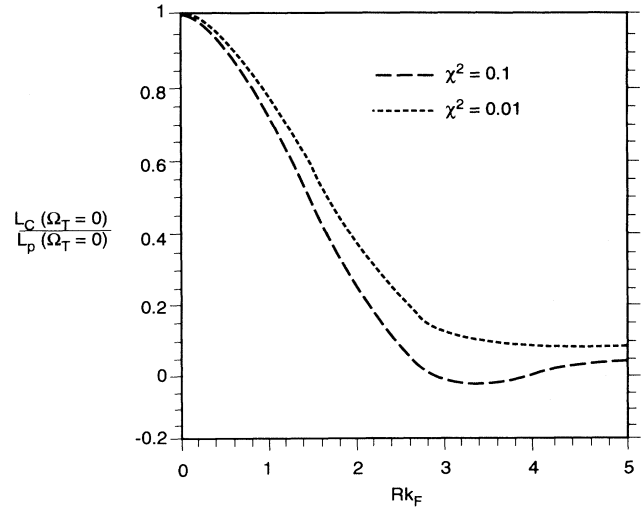
with

$$H(\chi^2) = \int_0^1 \frac{Z^6 dZ}{[Z^2 + \chi^2 f_1(Z,0)]^2}, \quad (34)$$

graphed in Fig. 3. Here we restrict to $\chi^2 \ll 1$, so we have $H(\chi^2) \cong \frac{1}{3}$.

For large interparticle distances, fulfilling $R \gg k_F^{-1}$, one gets through an integration by parts,

$$L_c(\Omega_T=0) \cong \frac{3}{2 \left[1 + \frac{\chi^2}{2} \right]^2} \left[\frac{V}{V_F} \right]^2 \frac{\cos(2k_F R)}{(2k_F R)^2}, \quad (35)$$

FIG. 4. Ratio of correlated to pointlike straggling $L_c(\Omega_{T=0})/L_p(\Omega_{T=0})$ [Eq. (32)] in the low-velocity regime.

which exhibits Friedel oscillations at $R \rightarrow \infty$.

The ratio $L_c(\Omega_{T=0})/L_p(\Omega_{T=0})$ derived from Eq. (32) with $L_c(\Omega_{T=0})$ obtained by putting $\text{sinc}(2k_F R Z) = 1$, is given on Fig. 4.

VI. CONCLUSIONS

We made use of the Born random-phase approximation [1,4,10] to investigate straggling of projectiles with pointlike and extended charges. Plasmon and binary collisions contributions have been given analytic expressions through a plasmon-pole approximation to the RPA dielectric function. Specific behaviors at high and low temperature are given analytic expressions. Diclusters randomly orientated with respect to projectile velocity have also been given a detailed treatment, which paves the way to further application in the field of particle-driven fusion.

ACKNOWLEDGMENTS

The Laboratoire de Physique des Gaz et des Plasmas is associé au CNRS.

- [1] A. Bret and C. Deutsch, Phys. Rev. E **47**, 1276 (1993).
- [2] C. Deutsch, Ann. Phys. (Paris) **1**, 111 (1986); Laser Part. Beams **2**, 449 (1984).
- [3] P. Nozières, *Le Problème A N Corps* (Dunod, Paris, 1964).
- [4] D. Pines and P. Nozières, *The Theory of Quantum Liquids* (Benjamin, New York, 1966).
- [5] J. K. Lindhard, K. Dan. Vidensk. Selsk. Mat. Fys. Medd. **28**, No. 8 (1964).

- [6] N. R. Arista and W. Brandt, Phys. Rev. A **23**, 1898 (1981).
- [7] G. Basbas and R. H. Ritchie, Phys. Rev. A **25**, 1943 (1982).
- [8] N. Arista, Phys. Rev. B **18**, 1 (1978).
- [9] I. Abril, M. Vicanek, A. Gras-Marti, and N. R. Arista, Nucl. Instrum. Methods Phys. Res., Sect. B **67**, 56 (1992).
- [10] G. Maynard and C. Deutsch, J. Phys. (Paris) **46**, 1113 (1985).